Acta Cryst. (1982). B**38**, 1921–1927

An Optical Transform Study of the Disorder in Dicalcium Barium Propionate

BY T. R. WELBERRY

Research School of Chemistry, Australian National University, PO Box 4, *Canberra, ACT* 2600, *Australia*

(*Received* 21 *October* 1981; *accepted* 9 *February* 1982)

Abstract

Optical transform methods are used to test the hypothesis of Stadnicka & Glazer [*Acta Cryst.* (1980), B**36**, 2977–2985], that the observed diffuse scattering from dicalcium barium propionate can be attributed to short-range order of the disordered propionate ions. Little evidence is found to support this view and evidence is presented that the diffuse scattering is largely attributable to distortions of the cation framework, in agreement with a later hypothesis put forward by Glazer, Stadnicka & Singh [*J. Phys. C* (1981), **14**, 5011–5029].

1. Introduction

There has recently been interest in the dicalcium metal propionates [$Ca_2M(C_2H_5COO)_6$ where M = metal] because of the existence of ferroelectricity and optical activity in some of their phases. Stadnicka & Glazer (1980) reported the crystal structure of the room-temperature form of dicalcium barium propionate (DBP) and found that the propionate groups were disordered. Moreover they observed diffuse scattering which they attributed to this disorder (static or dynamic). Subsequently Singh & Glazer (1981) reported detailed measurements of the diffuse scattering although did not significantly extend the earlier explanation of its origin. The initial aim of the present work was to test the hypothesis that the propionate disorder could explain the diffuse scattering and, more specifically, that the unusual contact distances between the C(2) and C(3) carbons on adjacent propionate groups provided the explanation for short-range order.

Subsequently, however, another crystal structure (dicalcium strontium propionate, DSP) was reported (Glazer, Stadnicka & Singh, 1981) and while this had obvious similarities to the DBP structure, it was no longer cubic. The major difference between the structures was that the cation framework had undergone distortions to result in a tetragonal structure. In this new light the authors suggested that similar distortions, but of a smaller magnitude, could exist in DBP since the refined calcium thermal parameters showed marked anisotropy in directions consistent with such a hypothesis.

In the sections that follow we make use of optical transform methods (Lipson, 1973) to test both hypotheses. We have previously used optical transform methods to interpret diffuse scattering effects in organic molecular crystals (Welberry & Jones, 1980). For the present problem the high symmetry and the number of different atomic species involved present difficulties not encountered previously. As a result we tackle the problem in the following way. In § 2 we consider the ordering of the propionates, and optical diffraction patterns are used in which only the light atoms C and O are represented. In § 3 we neglect the propionates and consider only the calcium–barium framework as the source of diffuse scattering.

2. The role of propionates in DBP disorder

The crystal structure refinement (Stadnicka & Glazer, 1980) assumed half occupancy of the 96(g) positions for O(1), O(2), C(1), C(2) and C(3) in the space group *Fd*3*m* (see *International Tables for X-ray Crystallography*, 1959). To describe the disorder we split the 96(g) positions into two groups which we label (1) and (2). These are chosen to ensure that only one of the two propionate orientations at each molecular site is generated when the fractional coordinates given in Table 1 are used, but otherwise the splitting is arbitrary. The orientation of propionates at individual sites is also labelled (1) or (2) according to which group is required

Table 1. *Fractional coordinates* (*after Stadnicka & Glazer*, 1980)

	x	y	z
Ba	0	0	0
Ca	$\frac{1}{8}$	$\frac{1}{8}$	$\frac{1}{8}$
O(1)	0·1447	0·0409	0·0409
O(2)	0·1663	−0·0386	−0·0386
C(1)	0·1869	0·0038	0·0038
C(2)	0·2710	0·0173	0·0173
C(3)	0·3193	−0·0228	−0·0228

0567-7408/82/071921-07$01.00

to generate it. Since both groups are required for cubic symmetry no perfectly ordered arrangement can exist with only one molecule per site. If the orientation of each propionate is decided arbitrarily then a statistically cubic distribution is achieved. However, we need to take into account short-range order and it is necessary to consider the molecular environment so that the cubic symmetry can be maintained statistically.

Each propionate has four contacts with each of two distinct types of neighbouring propionates. For each of these two types of contact (*A* and *B*) there are four different contact distances depending upon the orientation of the propionate itself and that of its neighbour. These contacts are typified by the C(3)–C(3) contact distances given in Table 2. It should be noted that the molecular orientation labels used are arbitrary and depend on which particular intermolecular contact is being considered. For a different pair of propionates it could well be the 1–2 orientation, that is 4·06 Å, for example. Fig. 1 shows a projection of that part of the disordered structure lying between $z = 0{\cdot}05$ and $z = 0{\cdot}30$. The *A*-type contacts are indicated by dotted lines and it is seen that these form isolated octahedra. In the cell shown examples of the three different *A* contact distances are evident. The *B* contacts provide a link between these closed octahedra. They are, for example, linked to the labelled C(3) atoms which form the apices of octahedra in the next layer. These *B* contacts are omitted for clarity. For short-range order to extend appreciable distances through the structure both *A* and *B* contacts must be considered.

Table 2. *Propionate contacts*

d_{cont} is the distance (Å) between C(3) atoms in neighbouring propionates

	Contact type *A*		Contact type *B*	
Molecular orientations	d_{cont}	Occurrence probability	d_{cont}	Occurrence probability
1–1	4·06	f_0	4·41	g_0
1–2	4·75	f_1	4·91	g_1
2–1	4·75	f_2	4·91	g_2
2–2	5·23	f_3	5·50	g_3

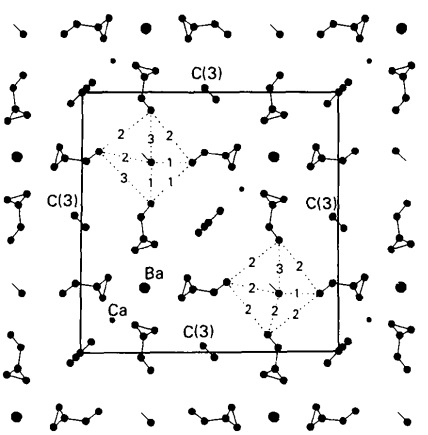

Fig. 1. The DBP structure. [100] projection of the region between $z = 0{\cdot}05$ and $z = 0{\cdot}30$, for a typical disordered unit cell. The contact distances shown between the C(3) atoms on neighbouring propionates are (1) 4·06, (2) 4·75, (3) 5·23 Å.

We can maintain statistical cubic symmetry by ensuring that the distribution of the contact distances is identical for each *A*-type contact irrespective of the particular propionate labels; and similarly for the *B*-type contacts. A requirement necessary for this is that $f_0 = f_3$ and $f_1 = f_2$, and similarly $g_0 = g_3$ and $g_1 = g_2$ (see Table 2). Note that in formulating the disorder in this way we have not precluded the possibility of two-dimensional ordered domains, as envisaged by Stadnicka & Glazer. Maintaining statistical cubic symmetry simply means that such domains are as likely to occur in each of the three equivalent directions. Since $\sum f_i = 1$ each contact type is subject to only one order parameter which for convenience we may take as, for example, f_0 *and* g_0. There are thus only four possible ordering schemes corresponding to the maximum and minimum values for f_0 and g_0.

We achieve such short-range ordering of propionates in a computer model of the disordered structure by use of Monte Carlo methods (Metropolis, Rosenbluth, Rosenbluth, Teller & Teller, 1953). We use a simplified method since we are only interested in obtaining a distribution as ordered as possible and not in the distribution at a particular temperature. Thus at each step in the Monte Carlo process we need only assess whether the orientation of the propionate chosen at random is to be preferred to its alternative. This we do by observing the number of 4·06 and 4·41 Å C(3)–C(3) contacts of the selected propionate with its eight neighbours and discriminate accordingly. For example if we wish to maximize the number of 4·06 and 4·41 Å contacts we put whichever propionate orientation gives the higher number of such contacts.

Our computer experiments were performed on a three-dimensional array of 30 × 30 × 4 unit cells with cyclic boundary conditions. These dimensions were dictated by the necessity to have a reasonably large two-dimensional sample for optical transform work and a small enough total size to allow for computer space and time. Since Singh & Glazer (1981) suggest the range of short-range order extends only over ~1–2 unit cells the dimensions chosen were considered to be the best compromise. We define a cycle of refinement as the number of Monte Carlo steps required to look at each propionate once on average (*i.e.* 172 800 steps). We found that starting from a random distribution about 30 cycles were required before the values for f_0, f_1 *etc.* became stationary. Iteration was continued for a further 70 cycles. Table 3 shows the resulting values of the f_i and g_i for the four possible ordering schemes.

Optical diffraction screens were obtained from the

Table 3. *Occurrence probabilities resulting from the Monte Carlo experiments for the four possible ordering schemes*

Distances energetically favoured	*A*-contact distances (Å)			*B*-contact distances (Å)		
	4·06	4·75	5·23	4·41	4·91	5·50
4·06/4·41	0·33	0·33	0·33	0·33	0·33	0·33
4·75/4·41	0·17	0·66	0·17	0·40	0·20	0·40
4·06/4·91	0·29	0·41	0·29	0·15	0·70	0·15
4·75/4·91	0·17	0·66	0·17	0·10	0·80	0·10
Random	0·25	0·50	0·25	0·25	0·50	0·25

final distributions using an Optronics P-1700 photomation system in a manner analogous to that described by Welberry & Jones (1980). A projection (down [100]) of the structure was used and only propionate atoms within one unit cell thickness were plotted to avoid problems of overlap. This is an approximation which in effect neglects correlation vectors which are out of plane by more than one unit cell. Since the range of order is expected to be only of the order of one cell repeat this is not a serious approximation in the present case. Each diffraction screen was made of a composite of the four layers of the total sample, placed side by side. This does not significantly affect the short-range-order diffuse scattering but does improve the diffraction patterns because of the reduced statistical fluctuations. Each screen therefore contained $\sim 8 \times 10^5$ atoms. The diffraction patterns of the four ordered lattices are shown in Fig. 2 together with that of the random distribution for comparison. The short-range order is difficult to discern in the screens themselves so in Fig. 3 we show plotted small samples of the distributions in which only the O(1) and O(2) atoms have been included. For propionates whose molecular axis lies approximately in the plane of the paper the carbon tails lie in a confused jumble within the differently shaped quadrilaterals

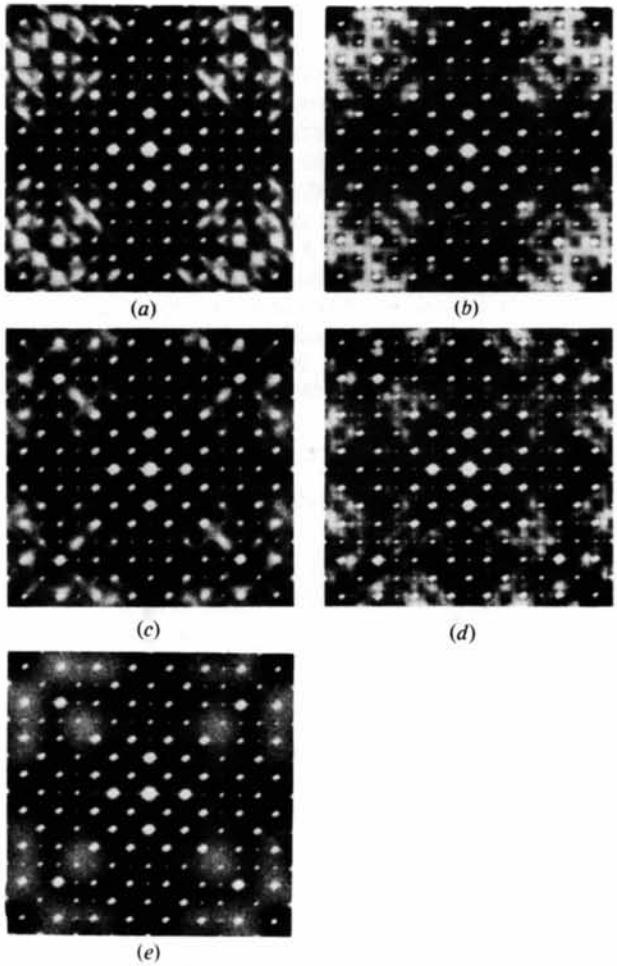

Fig. 2. Optical diffraction patterns of propionate distributions. Structures were ordered to maximize the number of C(3)–C(3) contacts with the lengths (Å) (*a*) 4·06 and 4·41, (*b*) 4·75 and 4·41, (*c*) 4·06 and 4·91, (*d*) 4·75 and 4·91. (*e*) The diffraction pattern of the random distribution, shown for comparison.

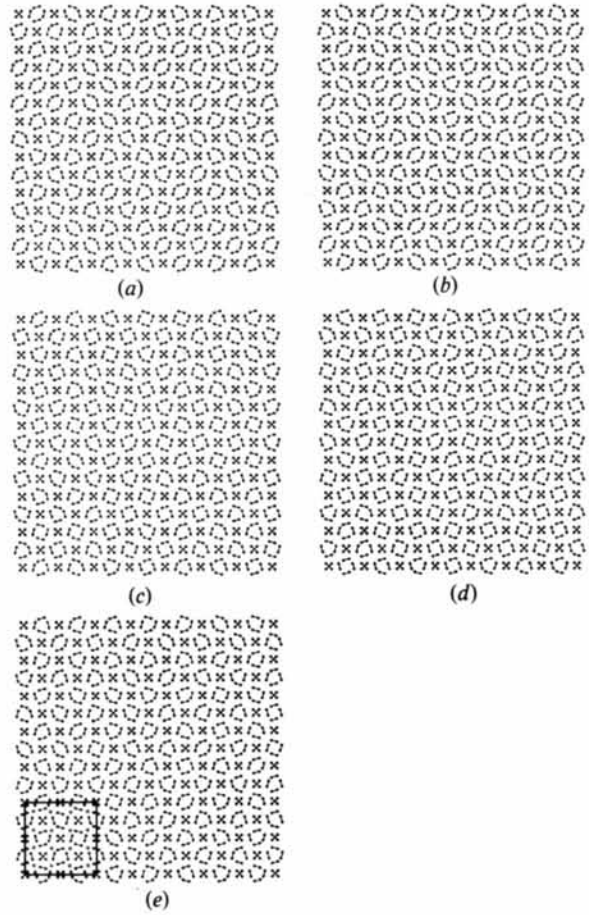

Fig. 3. Samples of the propionate distributions corresponding to the diffraction patterns of Fig. 2. Only the oxygen positions are shown here for clarity since the carbon tails of the propionates form a confused jumble within the quadrilaterals formed by four pairs of oxygens. The unit cell and the calcium sites are shown in (*e*).

made by the eight oxygens. Here the short-range order is evident in the shapes of these quadrilaterals.

While it is evident that considerable degrees of short-range ordering have been achieved by this simple Monte Carlo process it is also evident that there is little resemblance to the observed diffuse scattering, which we reproduce in Fig. 4. We may thus conclude that the observed diffuse scattering cannot be attributed to the ordering of propionates resulting from the direct inter-propionate interaction as described here. The arguments presented here have demonstrated that there are only four ways of ordering the propionates if the driving force is this short-range contact. We do not suggest that other ordering schemes could not produce other quite different propionate distributions. For example we might suggest that propionates could interact *via* O—O contacts or indirectly *via* the cations. However, the number of possibilities that might be tested is enormous and the Monte Carlo method used here is too time-consuming to make further systematic studies feasible.

One general feature of the diffraction patterns is perhaps worth mentioning. It is noticed that while for the disordered example, Fig. 2(*e*), the diffuse intensity is a fairly slowly varying function, the effect of correlation (see Fig. 2*a–d*) is to modify the intensity in a quite complex fashion with no clearly defined fringing system like that appearing in the observed data. This is evidently because of the complexity of the pattern of interatomic vectors contributing to the scattering due to many different orientations of the propionate groups within a cell. It seems unlikely, therefore, that any ordering scheme involving only the propionates could produce a scattering pattern as distinctive as that observed, and suggests that we turn our attention to the cation framework whose pattern of interatomic vectors is simple and distinctive.

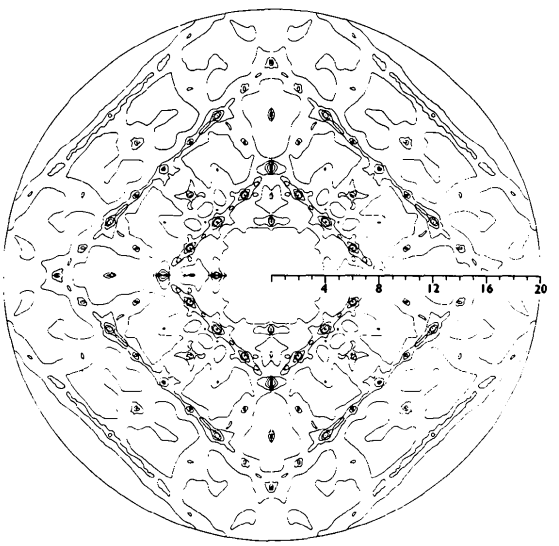

Fig. 4. The observed diffuse scattering data due to Singh & Glazer (1981).

3. The DSP structure as a model for disorder in DBP

Fig. 5(*a*) shows the projection of the cation framework in the paraelectric phase of dicalcium strontium propionate (DSP) as reported by Glazer *et al.* (1981). The figure demonstrates the relationship of the tetragonal unit cell to the cubic cell of DBP which would be derived by removing the cation-framework distortion. In this section we show how these regular distortions in DSP can be described in terms of a simple model and then how the parameters of the model may be changed to produce a disordered framework compatible with the observations made on the DBP structure. For simplicity we consider only the two-dimensional projection as shown in Fig. 5.

For convenience we use two subarrays of calcium ions which are depicted in Fig. 5(*b*). For subarray *A* (solid lines) we see that displacements are predominantly vertical, the displacement being about 14% of the mean subarray spacing, while for subarray *B* (dotted lines) the displacements are predominantly horizontal. We shall for the moment neglect the small displacements normal to these. *A* and *B* are identical but rotated by 90°. If we denote the displacement on one of these subarrays by X_{ij}, where i, j are indices defining the array, we can consider the array in terms of the correlations between neighbouring displacements. If the direction of displacement for subarray *A* is in the direction denoted by the index i we can define two correlation values C_T, C_L. With reference to Fig. 6:

$$C_T = \langle X_{ij} X_{i,j+1} \rangle / \langle X_{ij}^2 \rangle$$
$$C_L = \langle X_{ij} X_{i+1,j} \rangle / \langle X_{ij}^2 \rangle.$$

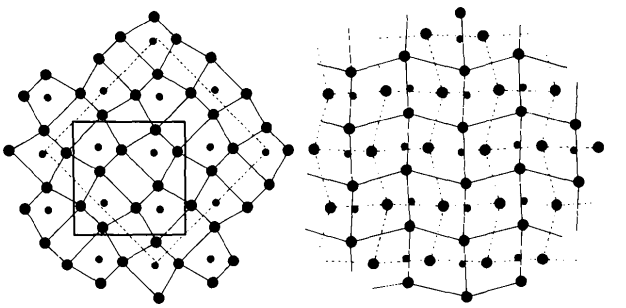

(*a*) (*b*)

Fig. 5. The cation framework in DSP. Large dots represent Ca and small dots represent Ba. (*a*) The DSP unit cell (indicated by heavy lines) and the related DBP cell (dotted lines). (*b*) The same region of structure as (*a*) with continuous lines indicating the sublattice *A* and dotted lines the sublattice *B* referred to in the text.

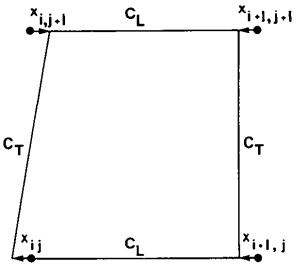

Fig. 6. The displacement variables, X_{ij}, and the associated correlation coefficients C_T and C_L used in the text.

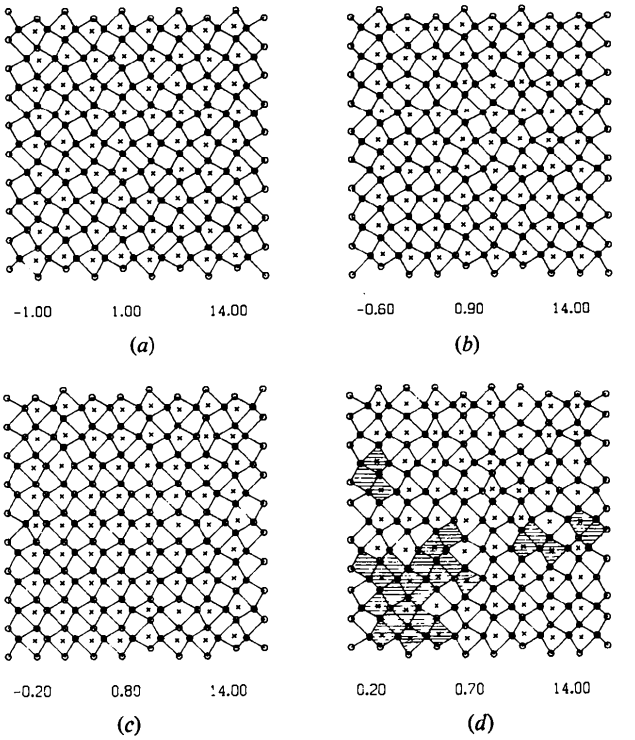

Fig. 7. Disordered cation frameworks. The figures beneath each drawing are the transverse correlation, the longitudinal correlation and the percentage displacement referred to in the text. (*a*) An idealized DSP structure, *cf.* Fig. 5.

The subscripts T and L refer to the fact that the correlations are in directions to which the displacements are transverse or longitudinal respectively. The same two correlations can be applied to the B array by maintaining the transverse and longitudinal nomenclature. The ordered DSP calcium framework is automatically produced when $C_T = -1{\cdot}0$ and $C_L = +1{\cdot}0$, *i.e.* transverse displacements are perfectly anti-correlated and longitudinal ones perfectly correlated. Strontium ions which are also displaced from their ideal DBP barium sites may be included by placing them at the centre of mass of the four surrounding calciums.

Using this idealized DSP model, we are now in a position to investigate the effect of allowing the correlation parameters to take non-unitary values and hence produce disordered cation frameworks in which the individual displacements nevertheless adhere to those observed in the DSP structure. To do this we make use of growth-disorder models as described, for example, in Welberry (1977) and Welberry & Carroll (1980) which enable rapid generation of disordered arrays containing specific correlation values. These models may be binary in which case the two values X_{ij} are used to represent positive or negative displacements, or Gaussian in which the X_{ij} are continuous variables normally distributed with zero mean and given variance. For the purposes of this paper binary variables have been used for convenience but very similar diffraction patterns would result with Gaussian variables, which might be more applicable if the disorder is fluctuating rather than static.

Rather than present a complete survey of the C_T, C_L space we show in Fig. 7 a sequence of arrays which vary from the ordered DSP structure to a disordered array which we judge represents a structure which gives a diffuse diffraction pattern best approximating the DBP data of Fig. 4. For these drawings we have maintained the magnitude of the displacements at a value comparable to that observed in DSP so that the relationship between the structures can be more readily assessed. However, for the corresponding diffraction screens from which diffraction patterns have been obtained we have used smaller displacements more comparable with those to be found in DBP. In DBP the cell edge of our A sublattice is 6·43 Å while the maximum r.m.s. displacement for the calcium is about 0·34 Å or about 5% of the subarray spacing. The diffraction patterns are shown in Fig. 8.

The final disordered array shown in Fig. 7(*d*) still contains recognizable features of the DSP structure which is characterized by the distinctive arrangement of squares, rectangles and trapezoids. Some such regions have been shaded to emphasize this point. The main difference between this structure and the ordered DSP is the replacement of the negative transverse correlation by a small positive one. The strong positive longitudinal correlation is only reduced to a small extent, its particular value being the parameter governing the sharpness of the diffuse-band profile measured by Singh & Glazer (1981). A positive value for the transverse correlation was considered appropriate since the intensity in the diffuse bands in Fig. 4 is not uniform along their length but tends to be greater close to Bragg spots than between them. This is akin to normal thermal diffuse scattering from acoustic phonons.

Although the distributions on the two subarrays A and B are required to be identical (but rotated by 90°) to maintain symmetry, we have in fact assumed them to be independent. This means that the DSP-type regions shown in Fig. 7(*d*) occur only when the two subarrays independently have the correct local form. It may be

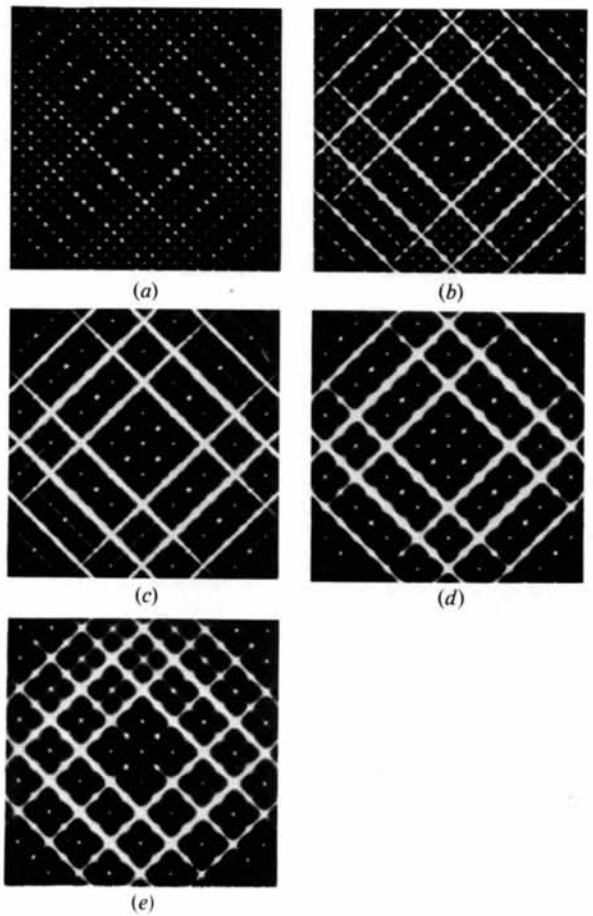

Fig. 8. Optical diffraction patterns of disordered cation frameworks. (*a*)–(*d*) correspond to distributions shown in Fig. 7 (*a*)–(*d*), but with displacements approximately one third as great. (*e*) The same distribution as (*d*) but with the addition of a transverse displacement (see text).

possible that by removing complete independence of the two subarrays these regions could occur more frequently than in the illustrations. It would be necessary that the dependence between the subarrays be *via* multi-point correlations in order to preserve the two-point correlations which give rise to diffraction properties. It may be possible in this way to preserve a greater proportion of more regularly shaped coordination polyhedra, but our methods using presently available stochastic models preclude an investigation of this possibility.

The diffraction pattern, Fig. 8(*d*), has many of the general features of the observed pattern of Fig. 4. It consists primarily of diffuse bands along the lines $h + k = 8n$ and the symmetry-related set $h - k = 8n$. One difference is that the scattering along the line $h + k = 0$ is zero for our simplified model since the displacements for the high correlation value which produces these fringes are purely longitudinal. The observed data do have this property at low angles, but at angles higher than the 440 reflection, for example, the $h + k = 0$ line can be clearly observed. This seems to indicate that a transverse component of displacement is required in addition to the longitudinal one used. This requires the introduction of a second variable, Y_{ij}, normal to X_{ij}. Note that such displacements are also to be found in the DSP structure, although they are of much smaller magnitude than X_{ij}. Fig. 8(*c*) shows the effect of including a transverse displacement with half the magnitude of the dominant longitudinal one, but with the same correlation values. Appreciable scattering on the $h + k = 0$ line is now observed.

A second point which must be mentioned is that there is some evidence for weak diffuse banding along the lines of $h + k = 8n + 4$, in particular $h + k = 20$. We found in our simple distortion model that these lines were more evident, the intensity being critically dependent on the relative scattering powers of the dots representing barium and calcium and on the relative magnitude of the displacements of these ions. Both of these quantities are difficult to specify precisely in our optical diffraction screens. The examples shown in Fig. 8 were taken from screens in which these parameters were adjusted to give minimal scattering on these lines.

The actual values of the correlations used were chosen somewhat arbitrarily, simply to demonstrate effects. Singh & Glazer (1981) report an order parameter for the main fringing system of $\alpha = 0{\cdot}124$. Their order parameter is related to our correlation coefficient by $C = 1{-}2\alpha$, but in fact refers to correlation between points on neighbouring (440) planes whereas our correlations refer to the subarrays A and B whose spacings correspond to neighbouring (220) planes. When this is taken into account the observed value of α is analogous to a correlation value of $C_L = 0{\cdot}56$ which corresponds to somewhat less order than in our Fig. 8(*d*) and (*e*).

While it was true to say that the examples involving the propionates only, that were discussed in § 2, gave diffraction patterns which were too intricately detailed and not sufficiently distinctive, this rather schematic model of the cation distortions is evidently too simple and cannot account for the detailed shape of the contours in Fig. 4. Nevertheless there seems little doubt that cation distortions of the sort described here must be the prime source of the observed scattering. To explain the detailed contour shapes inclusion of the propionate distribution would appear to be necessary.

4. Conclusion

While the results presented here do not suggest a mechanism for the disorder in DBP they provide evidence that the origin of the diffuse scattering

observed is in the distortion of the cation framework. Any contribution from the disorder of the propionate groups is secondary to this but not necessarily negligible. The actual distortions present have been shown to be compatible with the regular distortions present in the related DSP structure, though the actual magnitude is much less (approximately one third as large). This result provides substantial confirmation of the hypothesis of Glazer *et al.* (1981). Earlier Monte Carlo experiments to investigate whether the short-range ordering could be caused directly by the interaction between neighbouring propionate groups gave no support to that hypothesis and we must conclude that any mechanism must be related more directly to the cation framework.

I am grateful to Dr A. M. Glazer for suggesting this problem to me and for the use of the diffuse scattering data shown in Fig. 4, and to Dr J. Epstein with whom I have had fruitful discussions.

References

GLAZER, A. M., STADNICKA, K. & SINGH, S. (1981). *J. Phys. C*, **14**, 5011–5029.

International Tables for X-ray Crystallography (1959). Vol. II. Birmingham: Kynoch Press.

LIPSON, H. S. (1973). *Optical Transforms*. New York: Academic Press.

METROPOLIS, N., ROSENBLUTH, A. W., ROSENBLUTH, M. N., TELLER, A. H. & TELLER, E. (1953). *J. Chem. Phys.* **21**, 1087–1092.

SINGH, S. & GLAZER, A. M. (1981). *Acta Cryst.* A**37**, 804–808.

STADNICKA, K. & GLAZER, A. M. (1980). *Acta Cryst.* B**36**, 2977–2985.

WELBERRY, T. R. (1977). *Proc. R. Soc. London Ser. A*, **353**, 363–376.

WELBERRY, T. R. & CARROLL, C. E. (1980). *Acta Cryst.* A**36**, 921–929.

WELBERRY, T. R. & JONES, R. D. G. (1980). *J. Appl. Cryst.* **13**, 244–251.

Acta Cryst. (1982). B**38**, 1927–1931

Structure of Piperidinium Tris(pyrocatecholato)ferrate(III) Sesquihydrate

BY BRYAN F. ANDERSON,* DAVID A. BUCKINGHAM,† GLEN B. ROBERTSON‡ AND JOHN WEBB§

Research School of Chemistry, The Australian National University, PO Box 4, Canberra, ACT 2600, Australia

(*Received* 21 *October* 1981; *accepted* 8 *February* 1982)

Abstract

The structure of $(C_5H_{12}N)_3[Fe(C_6H_4O_2)_3].1{\cdot}5H_2O$ (M_r = 665·64) is reported. Crystals are monoclinic, space group $C2/c$ with a = 27·887 (4), b = 11·747 (1), c = 23·999 (3) Å, β = 118·19 (1)°, Z = 8, V = 6929·3 Å^3, $F(000)$ = 2848. Full-matrix least-squares refinement, with fixed H atoms, converged with R = 0·052 (3422 independent reflections). The anion is propeller shaped, with trigonally distorted octahedral coordination of the metal ion, and the piperidinium cations exhibit the chair conformation. The structure is extensively hydrogen bonded in sheets approximately perpendicular to [100]. It includes a large hydrophobic pocket which contains the 'half' water molecule and can accept small organic molecules giving rise to variable measured densities.

Introduction

Many of the iron-transport complexes known as siderophores exploit pyrocatechol (1,2-dihydroxybenzene) as the chelating group for binding Fe^{III} (Neilands, 1974). Interest in these complexes has stimulated several studies of the Fe^{III}–pyrocatechol system by a variety of techniques including crystallography (Raymond, Isied, Brown, Fronczek & Nibert, 1975; Anderson, Buckingham, Robertson, Webb, Murray & Clark, 1976). Elsewhere we have reported the structure of a dimeric complex, piperidinium μ-acetato-di-μ-pyrocatecholato-bis[(pyrocatecholato)ferrate-(III)], $(C_5H_{12}N)_3[(CH_3COO)\{Fe(C_6H_4O_2)_2\}_2]$, isolated from the Fe–pyrocatechol system under conditions of low base (Anderson, Webb, Buckingham & Robertson, 1982). In the present paper we report the structure of

* Present address: Department of Chemistry, Biochemistry and Biophysics, Massey University, Palmerston North, New Zealand.

† Present address: University of Otago, PO Box 56, Dunedin, New Zealand.

‡ To whom correspondence should be addressed.

§ Present address: School of Mathematical and Physical Sciences, Murdoch University, Murdoch, Western Australia 6150, Australia.

0567-7408/82/071927-05$01.00